



Adsorption of zinc (II) onto MnO₂/CS composite: equilibrium and kinetic studies

Dinh Van-Phuc^{a,*}, Le Ngoc-Chung^b, Nguyen Van-Dong^c, Nguyen Ngoc-Tuan^d

^aDong Nai University, 04 Le Quy Don Street, Tan Hiep Ward, Bien Hoa City, Dong Nai Province, Vietnam, email: dinhvanphuc82@gmail.com

^bDalat University, 01 Phu Dong ThienVuongstreet, Dalat City, Lam Dong Province, Vietnam, email: chungln@dlu.edu.vn

^cVNUHCM-University of Science, 227 Nguyen Van Cu Street, District 5, Hochiminh City, Vietnam.

^dNuclear Research Institute, Dalat, Lam Dong, Vietnam

Received 23 December 2015; Accepted 9 May 2016

ABSTRACT

In this work, manganese dioxide/chitosan (MnO₂/CS) was used to remove Zn(II) from an aqueous sample over a concentration range of 30–100 mg/L, adsorption time of 15–180 min, and pH of 2–5. The maximum sorption (>80%) was achieved at pH 4 after 80 min with an initial concentration of 50 mg/l and 0.1 g of MnO₂/CS. The experiment data were analyzed using the non-linear Freundlich, Langmuir, Redlich–Peterson, Sips, Temkin and Dubinin–Radushkevich (D–R) isotherm models. Langmuir isotherm offers maximum sorption capacity (q_m) of 24.21 mg/g (RMSE = 1.575 and $\chi = 0.8034$), while the Temkin and Dubinin–Radushkevich (D–R) isotherm models indicated that adsorption followed a physical process. Furthermore, kinetic studies showed that the adsorption processes partially followed the pseudo-second-order equation. In addition, intra-particle diffusion model was used to ascertain the sorption process mechanism. MnO₂/CS has also been used to remove Zn(II) from the wastewater produced by the galvanized iron manufacturing industry.

Keywords: MnO₂/chitosan composite; Adsorption; Zinc; Equilibrium; Kinetic; Galvanized iron

1. Introduction

Chitosan (CS), a biomaterial containing amine and hydroxyl groups, has been studied and used as a biosorption material to remove heavy metals from aqueous solution because it is nontoxic, biocompatible and environmentally friendly. However, its wide application is restricted due to its low surface area, poor mechanical properties and poor thermal stability. As a result, the tendency is to use physical/chemical modification to increase surface area as well as to improve mechanical stability.

Along with many types of crystalline structures, such as α -, β -, γ -, δ -..., manganese dioxide (MnO₂) has been extensively studied and applied to different areas as batteries [1–3],

catalysts [4–6] and adsorbents [7,8]. However, the application in adsorbents, especially the adsorption on heavy metals, is not as common as that in others.

Zinc is an essential element for plants, living organisms and human beings in trace amounts. However, it may cause serious health problems in high concentrations. Wastewater discharged from pharmaceuticals, and the galvanizing paints, pigments industries, and so on, is the main source of Zn(II) ions that endanger the natural environment and human life [9]. Of the physicochemical treatments, adsorption technology is considered to be one of the most efficient and promising for the treatment of trace amounts of heavy metal ions from large volumes of water. This is because of its high enrichment efficiency and the ease of phase separation. The use of

* Corresponding author.

CS [10–13], modified CS [11] and CS composites [14,15] as sorbents to remove Zn^{2+} ion from aqueous solution has been studied. However, the use of MnO_2 loaded CS nanoparticles as an adsorbent for Zn^{2+} ion has not been analyzed.

In this study, manganese dioxide/chitosan (MnO_2/CS) composite was used for the first time as a new adsorbent to remove Zn(II) ions from an aqueous sample. The influence of various experimental parameters on Zn^{2+} adsorption and the optimum adsorption conditions were studied. This paper also describes equilibrium and kinetics for the adsorption of Zn(II) onto MnO_2/CS composite material. Furthermore, MnO_2/CS was applied to remove Zn(II) ion from the wastewater produced by a private sector galvanized iron factory.

2. Materials and methods

2.1. Chemicals

Potassium permanganate ($KMnO_4$), ethyl alcohol (C_2H_5OH), nitric acid (HNO_3) and sodium hydroxide ($NaOH$) (Merck, Darmstadt, Germany) were used and a stock solution (1,000 mg/l) of Zn^{2+} was prepared using zinc nitrate in Milli-Q water (Merck, Darmstadt, Germany).

2.2. Instruments

Atomic absorption spectrophotometer AA-7000 (Shimadzu, Japan), a pH measurement (MARTINI Instruments Mi-150, Romania) calibrated using standardized HANNA buffer solutions (pH 4.01 ± 0.01 , 7.01 ± 0.01 , and 10.01 ± 0.01), temperature-controlled shaker (Model IKA R5), high resolution scanning electron microscopy S-4800 (FESEM-S4800, Hitachi) and surface area and porosity analysis (BET Micrometrics Gemini VII) were used.

2.3. Synthesis of MnO_2/CS composite material

MnO_2/CS composite was synthesized at the Institute for Environmental Studies, Dalat University, Vietnam [16]. A 300-mL solution of $KMnO_4$ was placed in the mixture of 12 g CS and 300 mL (C_2H_5OH and H_2O) and continuously stirred for 6 h. The solid product was washed several times with distilled water, and then dried at $60^\circ C$ for 12 h to retrieve the MnO_2/CS composite material.

2.4. Adsorption study

A 0.1-g MnO_2/CS composite was placed into a 100-mL conical flask containing 50 mL Zn^{2+} ion. The influences of pH (2–5), adsorption time (10–180 min) and metal ion concentration (30–100 mg/L) were studied.

A Shimadzu AA-7000 was used to determine the concentrations of the Zn^{2+} ion in the filtrate before and after the adsorption process. Adsorption capacity was calculated employing the mass balance equation for the adsorbent:

$$q = \frac{(C_o - C_e) \cdot V}{m} \quad (1)$$

where q is the adsorption capacity (mg/g) at equilibrium, and C_o and C_e are the initial concentration and the equilib-

rium concentration (mg/L), respectively. V is the volume (L) of solution and m is the weight (g) of adsorbent used.

During measurement on AAS, a QC standard was repeatedly checked after every 10 samples.

2.5. Removal of Zn^{2+} ion from wastewater sample

The wastewater sample was collected from a privately owned galvanized iron factory located in Bien Hoa City, Dong Nai Province, Vietnam. To study the possibility of removing Zn^{2+} ion, m (g) adsorbent ($m = 0.1$ – 2.0 g) was placed in 50 ml of the wastewater solution at pH = 4.0 with a shaking speed of 240 rpm. Furthermore, the volume of solution (50–500 ml) was also added to the conical flask containing 2.0 gram MnO_2/CS .

2.6. Data analysis and models' fitness

The equilibrium data were analyzed using the Freundlich, Langmuir, Sips, Redlich–Peterson, Temkin and Dubinin–Radushkevich isotherm expressions. All equilibrium model parameters were evaluated and optimized by non-linear regression using Excel 2010. For isotherm models used, some of their important characteristics such as the non-linear forms, their meaning and list of error functions are shown in Table 1.

3. Results and discussion

3.1. Characterization of MnO_2/CS [16]

In the SEM images (Fig. 1), the CS reveals a smooth and tight fracture surface, while MnO_2/CS exhibits a porous surface created by MnO_2 nanoparticles. This indicates that CS has been chemically modified and may offer more adsorption sites for adsorbate. The specific surface area (m^2/g) and pore volume distribution of CS, MnO_2 and MnO_2/CS were determined by BET and BJH-analysis (Table 2). The result showed that although MnO_2/CS and CS have mesopore, MnO_2/CS possesses a larger BET surface area ($15.75 m^2 \cdot g^{-1}$) than CS's, and this enables it to facilitate the enhancement in adsorption efficiency of Zn^{2+} compared with CS ($0.23 m^2/g$). It reveals that MnO_2 nanoparticles are possibly the main factor for the increase in the surface area of MnO_2 -loaded CS.

3.2. Factors affecting the adsorption of Zn^{2+}

3.2.1. pH

pH is an important factor which influences the adsorption of Zn(II) onto the MnO_2/CS surface. At low pH, the amine and carboxylic groups on CS are protonated, making them positively charged or neutral. As a result, Coulomb interaction force hinders the attraction of Zn^{2+} ion to functional groups on the sorbent. Moreover, the hydrogen ion which is of a larger size competes with metal ion, and consequently reduces the adsorption efficiency of the sorbent. At higher pH, Zn^{2+} ion forms hydroxo ion $ZnOH^+$ or/and insoluble hydroxide $Zn(OH)_2$ or zincate ZnO_2^{2-} that inhibits the adsorption of this ion. The adsorption efficiency of Zn^{2+} ion is maximized at pH value of approximately 4 (Fig. 2(a)). The increase in adsorption efficiency of Zn^{2+} ion may be explained by the fact that at pH 4, on the adsorbent surface, the $-NH_3^+$

Table 1
The non-linear, error functions and meaning of some models

| Isotherm | Non-linear form | Meaning | List of error functions |
|----------------------|---|--|--|
| Langmuir | $q_e = \frac{q_m \cdot K_L \cdot C_e}{1 + K_L \cdot C_e}$ | Estimating the maximum adsorption capacity corresponding to complete monolayer coverage on the MnO ₂ /CS material surface | $R^2 = 1 - \frac{\sum_{n=1}^n (q_{e,meas} - q_{e,calc})^2}{\sum_{n=1}^n (q_{e,meas} + q_{e,calc})^2}$ |
| Freundlich | $q_e = K_F \cdot C_e^{1/n}$ | Estimating the adsorption intensity of the adsorbate on the sorbent surface | |
| Sips | $q_e = \frac{K_S \cdot C_e^{1.5}}{1 + K_S \cdot C_e^{1.5}}$ | Estimating the agreement between Langmuir and Freundlich models | $RMSE = \sqrt{\frac{1}{n-1} \sum_{n=1}^n (q_{e,meas} - q_{e,calc})^2}$ |
| Redlich–Peterson | $q_e = \frac{K_{RP} \cdot C_e}{1 + K_{RP} \cdot C_e^2}$ | A hybrid isotherm featuring both Langmuir and Freundlich isotherms | $\chi^2 = \sum_{n=1}^n \frac{(q_{e,meas} - q_{e,calc})^2}{q_{e,calc}}$ |
| Temkin | $q_e = \frac{RT}{b_T} \ln(K_T C_e)$ | Evaluating the adsorption potentials of the adsorbent for adsorbates | The small values of RMSE and c ² indicate first a better model fit, and secondly, similarity of the model with the experimental data. |
| Dubinin–Radushkevich | $q_e = q_m \cdot e^{(-\beta \cdot \epsilon^2)}$ | Evaluating the value of mean sorption energy which gives information about chemical and physical sorption | |

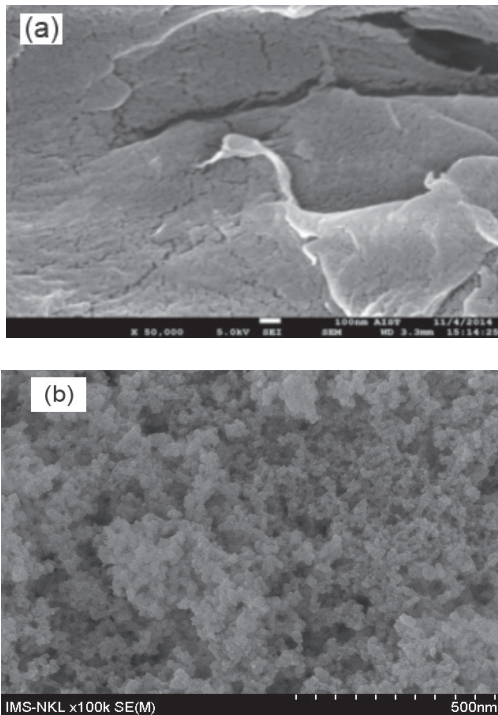


Fig. 1. SEM images of (a) CS and (b) MnO₂/CS.

Table 2
BET and BJH analysis results

| | Chitosan (CS) | MnO ₂ | MnO ₂ /CS |
|-------------|--------------------------------------|---------------------------------------|---------------------------------------|
| Pore size | 48.8 nm | 41.7 nm | 23.3 nm |
| BET surface | 0.23 m ² .g ⁻¹ | 65.00 m ² .g ⁻¹ | 15.75 m ² .g ⁻¹ |

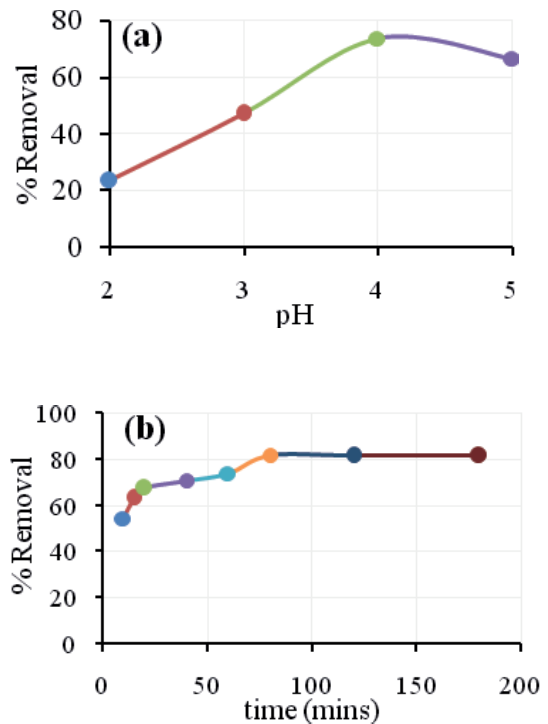


Fig. 2. Effects of (a) pH and (b) contact time on MnO₂/CS composite’s removal of zinc from water.

and carboxylic –COOH are deprotonated and become neutral and negatively charged. Consequently, the interaction between the newly formed groups and the positively charged metal cations occurred [17]. It can be concluded that the optimum pH for adsorption should be 4.0.

3.2.2. Adsorption time

The effect of contact time was studied at a room temperature of 24°C. The results show evidence that the adsorption of metal ions increased as contact time increased. The adsorption percentage of Zn(II) reached equilibrium after 80 min with 81.68% ($\pm 2.81\%$) adsorption of Zn(II) being recorded.

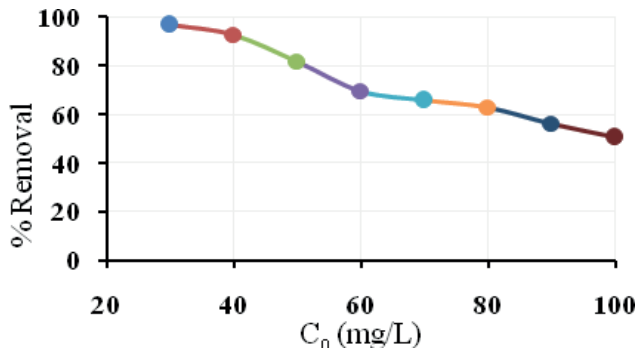


Fig. 3. Effect of initial concentration.

3.2.3. Initial concentration

Fig. 3 shows the influence of initial Zn²⁺ ion concentration on the adsorption by MnO₂/CS. It is clear that the percentage of zinc adsorbed decreased when the initial metal ion concentration increased. This fact reveals that all adsorbents have only a limited number of active sites and that the active sites lose their characteristics at higher concentrations of the Zn²⁺ ion due to the saturation of adsorption [18].

3.3. Equilibrium studies [10–28]

In this study, some two-parameter isotherm models (Langmuir, Freundlich and Temkin isotherms) and two three-parameter isotherm models (Redlich–Peterson, Sips and Dubinin–Radushkevich isotherms) served to assess the adsorption of zinc onto MnO₂/CS. The experimental data were fitted by non-linear modeling. The plots of fitted non-linear models are shown in Fig. 4 and the summarized parameters of these models are documented in Table 3.

All four isotherm models (Langmuir, Freundlich, Redlich–Peterson and Sips) were chosen to (1) estimate the

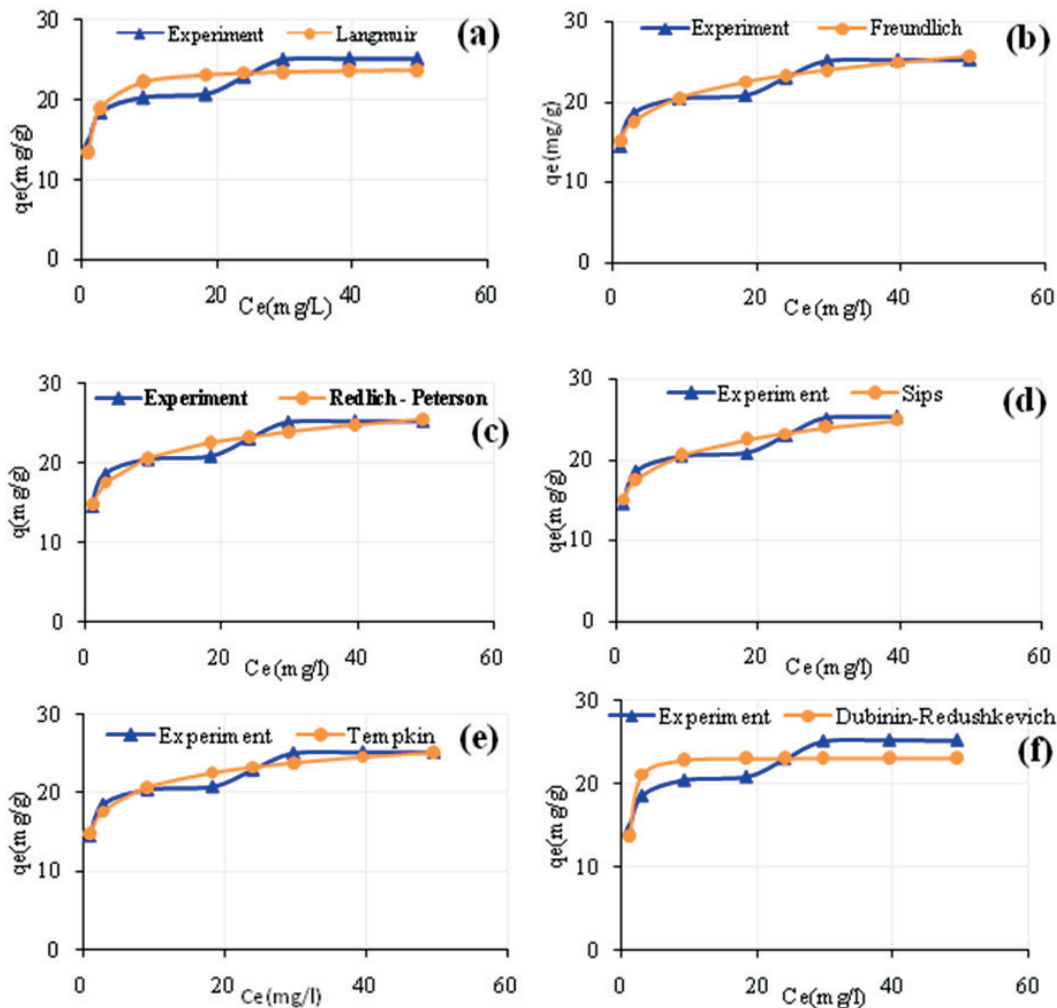


Fig. 4. Non-linear plots of (a) Langmuir, (b) Freundlich, (c) Redlich–Peterson, (d) Sips, (e) Temkin and (f) Dubinin–Radushkevich models.

Table 3
Equilibrium isotherm parameters

| Isotherm models | Parameters | |
|------------------|----------------|--------|
| Langmuir | K_L | 1.286 |
| | q_m (mg/g) | 24.21 |
| | RMSE | 1.575 |
| | R^2 | 0.8305 |
| | χ^2 | 0.8034 |
| Freundlich | $1/n$ | 0.1351 |
| | K_F | 15.12 |
| | RMSE | 0.9160 |
| | R^2 | 0.9426 |
| | χ^2 | 0.2813 |
| Sips | K_s | 15.61 |
| | α_s | 0.0339 |
| | β_s | 0.1413 |
| | RMSE | 0.9163 |
| | R^2 | 0.9426 |
| Temkin | χ^2 | 0.2808 |
| | K_T (L/mg) | 238.53 |
| | b_T (kJ/mol) | 0.9156 |
| | RMSE | 0.9340 |
| | R^2 | 0.9404 |
| Redlich–Peterson | χ^2 | 0.2839 |
| | K_R | 235.7 |
| | α_{KR} | 14.85 |
| | β_{KR} | 0.8782 |
| | RMSE | 0.9035 |
| D–R | R^2 | 0.9442 |
| | χ^2 | 0.0022 |
| | q_m (mol/g) | 23.08 |
| | β | 0.1732 |
| | E (kJ/mol) | 1.699 |
| | RMSE | 2.104 |
| | R^2 | 0.6975 |
| | χ^2 | 1.4275 |

maximum sorption capacity corresponding to complete monolayer coverage and (2) describe the distribution of the adsorbed specie between the liquid and solid phases, based on a set of assumptions that related to the heterogeneity/homogeneity of the solid surface. Results (see Table 3) showed that the sorption capacity (q_m) calculated from the Langmuir isotherm, which is a measure of the maximum sorption capacity corresponding to complete monolayer coverage, is 24.21 mg/g. The low Freundlich isotherm parameter $1/n$ value (0.1351<1) represents favorable sorption and confirms the heterogeneity of the adsorbent. Comparing the error functions, a coefficient of determination (R^2), the residual root mean square error (RMSE) and the chi-square test (χ^2) between the Langmuir and Freundlich models, it was observed that the data were

fitted with the Freundlich model as it produced high R^2 (0.9426), low RMSE (0.9426) and small χ^2 (0.2813) values. However, the value of R^2 (0.9426), RMSE (0.9163) and χ^2 (0.2808) calculated by the Sips isotherm model revealed that adsorption Zn(II) onto MnO₂/CS surface followed both the Langmuir and Freundlich isotherm models. In addition, the value of smallest χ^2 (0.0022) and highest R^2 (0.9442) calculated from the Redlich–Peterson isotherm model also demonstrated that this isotherm model gave the best fit.

The Temkin and Dubinin–Radushkevich isotherm models were chosen to firstly estimate the heat of adsorption, and second determine the type of sorption (physical or chemical) based on the mean free energy. The Temkin isotherm equation assumes that the heat of adsorption of all the molecules in a layer decreases linearly with coverage due to adsorbent-adsorbate interactions, and that the adsorption is characterized by a uniform distribution of the bonding energies, up to some maximum binding energy. The Temkin constant, b_T , related to heat of sorption for Zn²⁺ ion was 0.9156 kJ/mol. This low value in our study indicated a weak interaction between the adsorbed specie and adsorbent, thus supporting the assumption that a physical adsorption process is the dominant one in the present study [22]. Likewise, the value of mean sorption energy provides useful information about chemical and physical sorption. For example, an E value within 1/8 kJ/mol indicates the physical sorption; within 8/16 kJ/mol for ion-exchange and more than 16 kJ/mol for chemical sorption [23,27,28]. The value of mean sorption energy, E (kJ/mol), can be calculated from D–R parameter β as follows:

$$E = \frac{1}{\sqrt{-2\beta}} \quad (2)$$

In this study, the E value (1.699 kJ/mol) was less than 8 kJ/mol, indicating that the type of sorption of Zn²⁺ ion on MnO₂/CS composite is essentially physical.

3.4. Kinetic studies [10–28]

3.4.1. Pseudo-first-order and pseudo-second-order models

To study kinetics, the adsorption data were analyzed using different kinetic models, namely the pseudo-first-order and pseudo-second-order models (Fig. 5 and Table 4). The kinetic parameters, which are helpful for predicting the adsorption rate, provide important information for designing and modeling the processes. The results showed that the theoretical q_e value (21.10 mg/g) with high correlation coefficient ($R^2 = 0.9990$) calculated from the pseudo-second-order kinetic model was found to be closer to the experimental value, q_e (exp) (21.50 mg/g), than the value (5.985 mg/g) estimated from the first-order kinetic model. This may indicate that the pseudo-second-order adsorption mechanism was predominant for adsorption of Zn(II) by MnO₂/CS composite. The pseudo-first-order and pseudo-second-order kinetics rate constants for the adsorption of Zn(II) ion on MnO₂/CS were shown in Table 4.

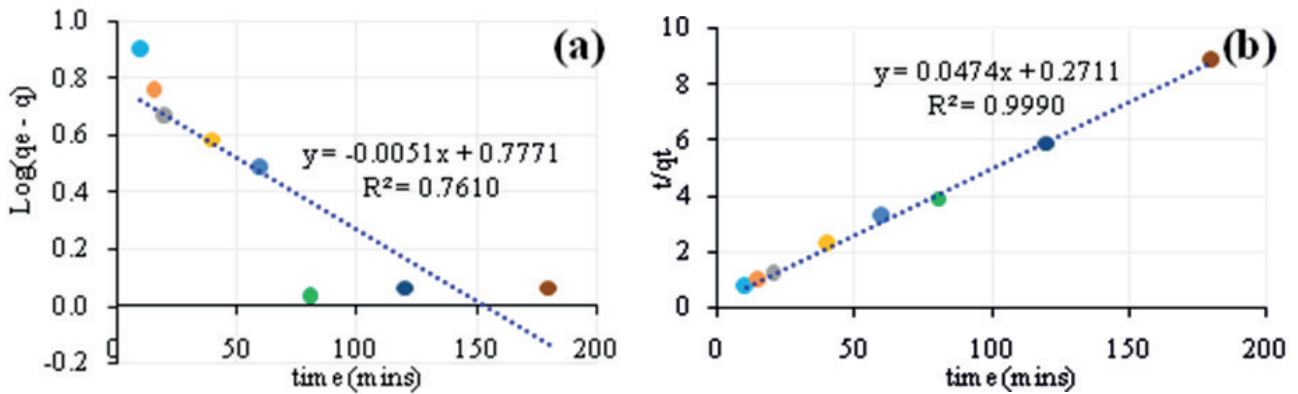


Fig. 5. (a) Pseudo-first-order kinetic plot and (b) pseudo-second-order kinetic plot for the adsorption of Zn²⁺ ion onto MnO₂/CS.

Table 4
Kinetic parameters

| Kinetic models | At boundary conditions: $q = 0$ to $q = q_t$ at $t = 0$ to $t = t$ | | Kinetic parameters (at $C_0 = 50$ ppm) | |
|--------------------------------|---|---|--|------------------------|
| | | | q_e (exp) (mg/g) | 21.50 |
| Pseudo-first-order model | $\frac{dq}{dt} = k_1(q_e - q)$ | $\log(q_e - q_t) = \log q_e - \frac{k_1 t}{2,303}$ | K_1 (min ⁻¹) | 0.01175 |
| | | | R^2 | 0.7610 |
| Pseudo-second-order model | $\frac{dq}{dt} = k_2(q_e - q)^2$ | $\frac{t}{q} = \frac{1}{k_2 q_e^2} + \left(\frac{1}{q_e}\right)t$ | q_e (cal) (mg/g) | 5.985 |
| | | | K_2 (g.mg ⁻¹ .min ⁻¹) | 6.091.10 ⁻⁴ |
| | | | h (mg/g.min) | 0.2711 |
| | | | R^2 | 0.9990 |
| Intra-particle diffusion model | | $q_t = k_d t^{1/2} + C$ | q_e (cal) (mg/g) | 21.10 |
| | | | K_{d1} | 0.4475 |
| | | | K_{d2} | 0.0396 |
| | | | K_{d3} | -0.0008 |

3.4.2. Intra-particle diffusion model

Intra-particle diffusion model is commonly used to identify the diffusion mechanism involved in the adsorption process, which the pseudo-first-order and pseudo-second-order kinetic models cannot determine. The model was developed by Weber and Morris based on the following equation for the rate constant:

$$q_t = k_d t^{1/2} + C \tag{3}$$

where q_t is the quantity of metal ions adsorbed at time t (mg.g⁻¹), k_d the initial rate of intra-particle diffusion (mg.L⁻¹.min^{-1/2}), and C is the y-intercept which is proportional to the boundary layer thickness.

Fig. 6 shows that the uptake of Zn²⁺ ion on the MnO₂/CS surface included three stages. The first one is an instantaneous adsorption stage in which Zn²⁺ ion was transferred from solution to the material surface. The second part is a gradual adsorption stage, where the intra-particle diffusion is the controlling factor. The third part constitutes the final equilibrium stage where the intra-particle diffusion

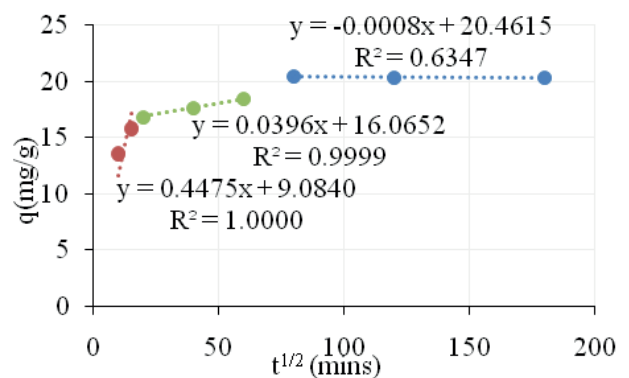


Fig. 6. Plot of the intra-particle diffusion kinetic for adsorption Zn²⁺ onto MnO₂/CS.

starts to decelerate due to, firstly, extremely low Zn²⁺ ion concentrations in the solution, and secondly, a decrease in the number of adsorption sites [19]. The intra-particle diffusion constants for all three stages (k_{d1} , k_{d2} , k_{d3}) are given in Table 4.

Table 5
Comparison of maximum sorption capacity of Zn^{2+} ion by some composite materials

| Materials | pH | q_m (mg/g) | References |
|--|-----|--------------|------------|
| Chitosan | 7.0 | 1.210 | [10] |
| Chitosan | – | 10.32 | [11] |
| Cross-linked chitosan with epichlorohydrin | – | 10.21 | [11] |
| Chitosan | 6.0 | 47.15 | [12] |
| Chitosan | 8.0 | 29.90 | [13] |
| Chitosan (Chitin)/cellulose composite | 5.8 | 19.70 | [14] |
| Non-cross-linked chitosan-coated montmorillonite beads | 4.0 | 13.49 | [15] |
| Cross-linked chitosan-coated montmorillonite beads | 4.0 | 14.71 | [15] |
| Chitosan | 4.0 | 6.95 | This study |
| MnO_2 | 4.0 | 55.23 | This study |
| MnO_2/CS composite | 4.0 | 24.21 | This study |

3.5. Comparison with other studies

The adsorbent's applicability depends on the adsorption capacity, specific surface area, ease of use, availability, cost and effect on the environment. In this study, the maximum adsorption capacity for Zn^{2+} ion (calculated from the Langmuir isotherm model) with other parameters obtained from MnO_2/CS composite and other adsorbents are compared (Table 5). As a result, it could be concluded that the adsorptivity of MnO_2/CS composite on zinc from water is more efficient than almost other CS-based adsorbents. Furthermore, it is clear that loading MnO_2 onto promoted the capacity of CS more than 3.5 times at the same condition from 6.95 mg/g to 24.21 mg/g even though there was only approximately 15% of MnO_2 loaded on the surface of CS (Fig. 7).

3.6. Application to remove zinc from the wastewater

Table 6 shows pH value and initial Zn^{2+} ion concentration of the wastewater sample as well as the possibility of adsorption Zn^{2+} ion onto MnO_2/CS material. Results indicated that 99.87% adsorption of $Zn(II)$ was recorded with 50 mL solution per 2.0 g material. In addition, 2.0 g material could remove over 90% from 500 mL of wastewater solution. From these findings, it is clear that MnO_2/CS is a good material for removing Zn^{2+} ion from the wastewater produced by the galvanized iron factory.

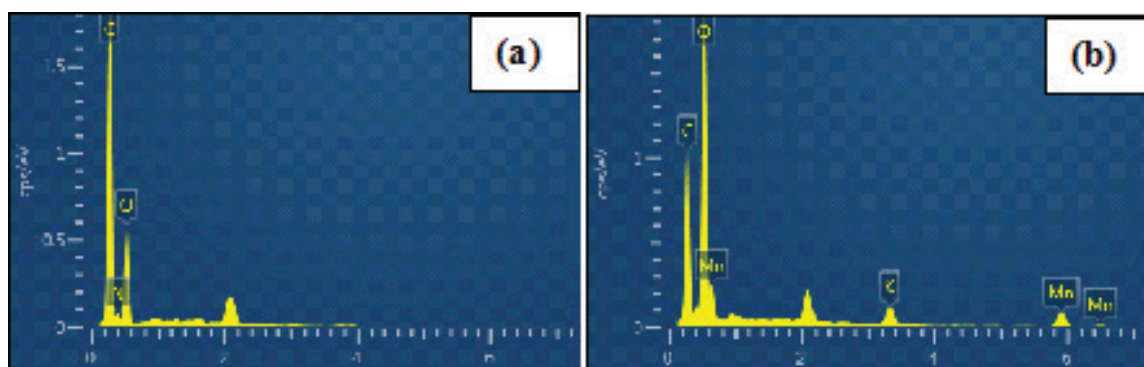


Fig. 7. EDX images of (a) CS and (b) MnO_2/CS .

Table 6
Effectiveness of MnO_2/CS material on the removal of $Zn(II)$ ion in wastewater

| | Before C_0 (mg/l) | m (g) | V (mL) | % Removal | SD ($n = 6$) | RSD ($n = 6$) | |
|----------|------------------------|------------|-------------|-----------|-------------------|--------------------|------|
| pH = 5.6 | 175.00 | 0.1 | 50 | 32.37 | 0.0298 | 5.44 | |
| | | 0.2 | | 49.81 | 0.0183 | 4.59 | |
| | | 0.5 | | 92.47 | 0.0034 | 1.15 | |
| | | 1.0 | | 99.48 | 0.0105 | 1.28 | |
| | | 2.0 | | 99.87 | 0.0079 | 3.62 | |
| | 175.00 | 2.0 | 100 | 99.36 | 0.0086 | 7.67 | |
| | | 175.00 | | 150 | 99.08 | 0.0057 | 3.52 |
| | | | | 200 | 94.82 | 0.0058 | 0.64 |
| | | | | 300 | 94.72 | 0.0044 | 0.47 |
| | | | | 500 | 92.86 | 0.0061 | 0.97 |

4. Conclusions

In this study, MnO₂/CS composite was used as an adsorbent to remove Zn²⁺ from an aqueous solution in optimal conditions (pH = 4, time = 80 min and shaking speed = 240 rpm). Using the Langmuir isotherm, the adsorption capacity for Zn²⁺ ion was found to be 24.21 mg/g. Calculating from Temkin and D–R isotherms revealed that the type of sorption of Zn(II) on MnO₂/CS is essentially physical. Kinetic studies showed that the adsorption processes followed the pseudo-second-order model. Furthermore, Zn(II) from the wastewater collected at a galvanized iron manufacturing business was removed with H > 90% (for initial concentration range of 175 ppm) by the adsorption onto MnO₂/CS.

Symbols

| | | |
|---------------|---|---|
| b_T | — | Temkin isotherm constant |
| C_e | — | the equilibrium concentration, mg/L |
| E | — | mean free energy, kJ/mol |
| K_F | — | Freundlich constant |
| K_L | — | Langmuir constant |
| K_{RL} | — | Redlich–Peterson isotherm constant, L/g |
| K_S | — | Sips constant |
| K_T | — | Temkin isotherm equilibrium binding constant, L/g |
| n | — | adsorption intensity |
| q_e | — | the adsorption capacity at equilibrium, mg/g |
| q_m | — | the maximum adsorption capacity, mg/g |
| R^2 | — | correlation coefficient |
| RMSE | — | Root mean square error |
| α_{RP} | — | Redlich–Peterson isotherm constant, 1/mg |
| α_s | — | Sips isotherm model constant, L/mg |
| β | — | Dubinin–Radushkevich isotherm constant, mol ² /kJ ²) |
| β | — | Redlich–Peterson isotherm exponent |
| β_s | — | Sips isotherm model exponent |
| ε | — | Dubinin–Radushkevich isotherm constant |
| χ | — | Non-linear chi-square test |

References

- M.M. Thackeray, Manganese oxides for lithium batteries, *Prog. Solid State Chem.*, 25 (1997) 1–71.
- Y. Yanyan, X. Lifan, Z. Yanqiang, W. Fengyun, Hydrothermal synthesis and electrochemical characterization of α -MnO₂ nanorods as cathode material for lithium batteries, *Int. J. Electrochem. Sci.*, 3 (2008) 67–74.
- J. Li, B. Xi, Y. Zhu, Q. Li, Y. Yan, Y. Qian, A precursor route to synthesize mesoporous γ -MnO₂ microcrystals and their applications in lithium battery and water treatment, *J. Alloy Compd.*, 509 (2011) 9542–9548.
- Z. Yang, Y. Zhang, W. Zhang, X. Wang, Y. Qian, X. Wen, S. Yang, Nanorods of manganese oxides: synthesis, characterization and catalytic application, *J. Solid State Chem.*, 179 (2006) 679–684.
- X. Fu, J. Feng, H. Wang, K.M. Ng, Manganese oxide hollow structures with different phases: synthesis, characterization and catalytic application, *Catal. Commun.*, 10 (2009) 1844–1848.
- M. Sun, B. Lan, L. Yu, F. Ye, W. Song, J. He, G. Diao, Y. Zheng, Manganese oxides with different crystalline structures: facile hydrothermal synthesis and catalytic activities, *Mater. Lett.*, 86 (2012) 18–20.
- Q. Huo, H. Xiao, Synthesis of MnO₂ nanowires and its adsorption property to lead ion in water, *J. Chem. Pharm. Res.*, 6 (2014) 270–275.
- L. Ngoc Chung, D. Van Phuc, Sorption of lead (II), cobalt (II) and copper (II) ions from aqueous solutions by γ -MnO₂ nanostructure, *Adv. Nat. Sci.: Nanosci. Nanotechnol.*, 6 (2015) 025014.
- A.K. Bhattacharya, S.N. Mandal, S.K. Das, Adsorption of Zn(II) from aqueous solution by using different adsorbents, *Chem. Eng. J.*, 123 (2006) 43–51.
- G. Karthikeyan, K. Anbalagan, N. Muthulakshmi Andral, Adsorption dynamics and equilibrium studies of Zn(II) onto chitosan, *J. Chem. Sci.*, 116 (2004) 119–127.
- A.-H. Chen, S.-C. Liu, C.-Y. Chen, C.-Y. Chen, Comparative adsorption of Cu(II), Zn(II), and Pb(II) ions in aqueous solution on the crosslinked chitosan with epichlorohydrin, *J. Hazard. Mater.*, 154 (2008) 184–191.
- M. Benavente, L. Moreno, J. Martinez, Sorption of heavy metals from gold mining wastewater using chitosan, *J. Taiwan Inst. Chem. E.*, 42 (2011) 976–988.
- T. Budnyak, V. Tertykh, E. Yanovska, Chitosan immobilized on silica surface for wastewater treatment, *J. Mater. Sci. (Medžiagotyra)*, 20 (2014) 177–182.
- X. Sun, B. Peng, Y. Ji, J. Chen, D. Li, Chitosan(chitin)/cellulose composite biosorbents prepared using ionic liquid for heavy metal ions adsorption, *AIChE J.*, 55 (2009) 2062–2069.
- W.-C. Tsai, S. Ibarra-Buscano, C.-C. Kan, C. Morales Futralan, M.L.P. Dalida, M.-W. Wan, Removal of copper, nickel, lead, and zinc using chitosan-coated montmorillonite beads in single- and multi-metal system, *Desal. Wat. Treat.*, 57 (2016) 9799–9812.
- L. Ngoc-Chung, D. Van-Phuc, N. Ngoc-Tuan, Synthesis and characterization of MnO₂ nanoparticles loaded onto chitosan and its application in Pb²⁺ adsorption, In: *Proceedings of the Third Intl. Conf. on Advances in Applied Science and Environmental Engineering*, ASEE, Malaysia (2015) 27–31.
- A. Heidari, H. Younesi, Z. Mehraban, H. Heikkinen, Selective adsorption of Pb(II), Cd(II), and Ni(II) ions from aqueous solution using chitosan–MAA nanoparticles, *Int. J. Biol. Macromol.*, 61 (2013) 251–263.
- W.-T. Tsai, H.-R. Chen, Removal of malachite green from aqueous solution using low-cost chlorella-based biomass, *J. Hazard. Mater.*, 175 (2010) 844–849.
- F.-C. Wu, R.-L. Tseng, R.-S. Juang, Comparative adsorption of metal and dye on flake- and bead-types of chitosans prepared from fishery wastes, *J. Hazard. Mater.*, 73 (2000) 63–75.
- M.E. Argun, S. Dursun, C. Ozdemir, M. Karatas, Heavy metal adsorption by modified oak sawdust: thermodynamics and kinetics, *J. Hazard. Mater.*, 141 (2007) 77–85.
- K.Y. Foo, B.H. Hameed, Insights into the modeling of adsorption isotherm systems, *Chem. Eng. J.*, 156 (2010) 2–10.
- J. Anwar, U. Shafique, Z. Waheed uz, M. Salman, A. Dar, S. Anwar, Removal of Pb(II) and Cd(II) from water by adsorption on peels of banana, *Bioresour. Technol.*, 101 (2010) 1752–1755.
- S. Vasiliu, I. Bunia, S. Racovita, V. Neagu, Adsorption of cefotaxime sodium salt on polymer coated ion exchange resin microparticles: kinetics, equilibrium and thermodynamic studies, *Carbohydr. Polym.*, 85 (2011) 376–387.
- J.C. Igwe, A.A. Abia, C.U. Sonde, Pseudo-kinetics and intraparticle diffusion models for sorption of Zn(II), Cd (II) and Pb (II) ions onto maize cob, *ABSU J. Environ. Sci. Technol.*, 1 (2011) 25–36.
- M.A. Hossain, H.H. Ngo, W.S. Guo, T. Setiadi, Adsorption and desorption of copper(II) ions onto garden grass, *Bioresour. Technol.*, 121 (2012) 386–395.
- P. Salaryan, M. Noroozifar, H. Atashi, S.M. Sajadi, F. Mokari, H. Salaryan, Removal of manganese from petrochemical effluent using black carbon: isotherm and kinetic studies, *Int. J. Chem. Biochem. Sci.*, 3 (2013) 110–119.
- R.R. Bhatt, B.A. Shah, Sorption studies of heavy metal ions by salicylic acid–formaldehyde–catechol terpolymeric resin: isotherm, kinetic and thermodynamics, *Arab. J. Chem.*, 8 (2015) 414–426.
- H. Javadian, F. Ghorbani, H.-A. Tayebi, S.H. Asl, Study of the adsorption of Cd (II) from aqueous solution using zeolite-based geopolymer, synthesized from coal fly ash; kinetic, isotherm and thermodynamic studies, *Arab. J. Chem.*, 8 (2015) 837–849.